Robust adjustment of a geodetic network measured by satellite technology in the Dargovských Hrdinov suburb

Slavomír Labant[1], Gabriel Weiss and *Pavel Kukučka*

This article addresses the adjustment of a 3D geodetic network in the Dargovských Hrdinov suburbs using Global Navigation Satellite Systems (GNSS) for the purposes of deformation analysis. The advantage of using the GNSS compared to other terrestrial technology is that it is not influenced by unpredictability in the ground level atmosphere and individual visibilities between points in the observed network are not necessary. This article also includes the planning of GNSS observations using Planning Open Source software from Trimble as well as subsequent observations at individual network points. The geodetic network is processing on the basis of the Gauss-Markov model using the least square method and robust adjustment. From robust methods, Huber's Robust M-estimation and Hampel's Robust M-estimation were used. Individual adjustments were tested and subsequently the results of analysis were graphically visualised using absolute confidence ellipsoids.

***Keywords:** GNSS, 3D geodetic network, planning observations, robust adjustment.*

Introduction

The term "Global Navigation Satellite Systems" (GNSS) is used to describe navigation satellite systems with worldwide coverage, allowing determination of position, speed and time, and they continuously meet the requirements of potential users in the civilian sphere. At present, there are four GNSS in operation and under development and four regional navigation systems (Tab. 1). However, not all are fully functional and their current operational and development status is shown in Tab. 1.

Tab. 1: *Operational status of selected current navigation satellite systems.*

		Name	Country	Status
Navigation satellite systems	Global	GPS	USA	in operation
		GLONASS	USSR/Russia	function with limitations
		Galileo	EU	under development with global coverage by 2014
		Compass	China	under development with global coverage by 2017
	Regional	BeiDou 1	China	in operation
		DORIS	France	in operation
		IRNSS	India	under development
		QZSS	Japan	under development

GNSS assist in improving the accuracy of various supporting satellite systems within SBAS (Sattelite Based Augmentation System), where the most significant are:
- EGNOS (European Geostationary Overlay Service),
- WAAS (Wide Area Augmentation),
- MSAS (Multi – Fuction Transport Sattelite Augmentation System).

Within Slovakia, permanent GNSS services are used for geodetic measurements:
- SKPOS,
- Leica SmartNet.

Planning GNSS observations

Maximum accuracy of a position which can be achieved is limited by the geometry of the GNSS satellites. Errors in the GNSS receiver position are caused by two factors: the geometry of satellites in the entire sky and the accuracy with which the distance to each GNSS satellite is known. The factor of satellite geometry is sometimes represented as a numeric value known as "Dilution of Precision" (DOP). The higher the DOP, the greater the possible error in the precision of determining a position. GNSS receivers in construction devices

---

[1] *Ing. Slavomír Labant, PhD., Prof. Ing. Gabriel Weiss, PhD., Ing. Pavel Kukučka, PhD.,* Institute of Geodesy, Cartography and Geographic Information Systems, BERG Faculty, Technical University of Košice, Letná 9, 042 00 Košice, Slovak Republic, slavomir.labant@tuke.sk, gabriel.weiss@tuke.sk, pavel.kukučka@tuke.sk

(e.g. graders) often come with software which displays the actual DOP. If the value is too high, it prevents proceeding in work which depends upon this measurement. GNSS receivers usually do not display the DOP but instead, they display a general index of positional unpredictability (different producers of receivers - different definition).

Planning of GNSS observations is carried out using software, for example, Planning (Fig. 1) from Trimble which is freely downloadable, and open source [9]. It is a small, useful utility which assists in selecting a suitable time period for observation using GNSS receivers.

The latest version of Planning software is 2.9 which has:

- improved support of the Galileo system,
- improved support of the Compass,
- Glonass support for importing SSF almanac,
- an updated list of WAAS satellites.

For correct planning of GNSS observations, it is necessary to always have an imported file with the latest ephemerides (almanac.alm). After determining the planned position for the GNSS receiver, the date, time and length of observation, it is possible to display a "Number of Satellites" graph (Fig. 2), which displays the number of satellites, particularly GPS, are visible under the assumption that the view of the sky is clear. In the software, it is possible to set the position and height of obstacles which obscure the view of the sky and this fact will be reflected in the display of number of visible satellites.
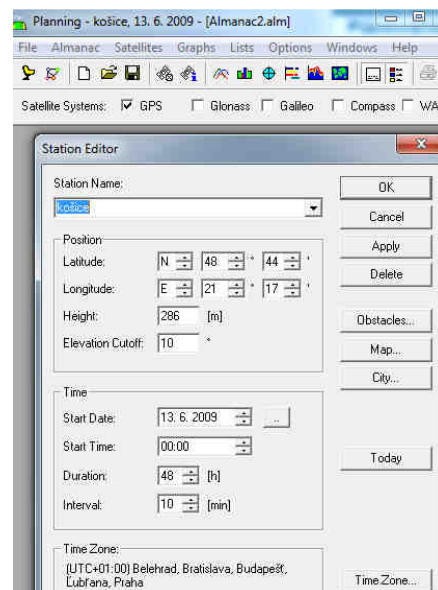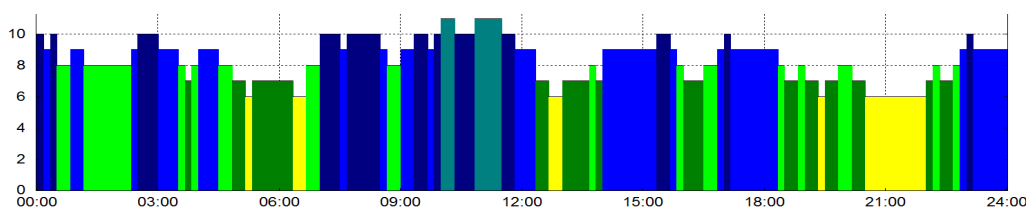

Fig. 1 Planning 2.9 software.

Fig. 2 Display of the number of GPS satellites during daytime.

This software also provides information about DOP values in graphic form (Fig. 3), where it takes into account the number of satellites as well as movement in the sky. 5 types of DOPs [10]:

- GDOP - geometric (including movement and 3D position),
- PDOP - position in space (3D positions for a stationary observer),
- HDOP - horizontal (2D, without altitude above sea level),
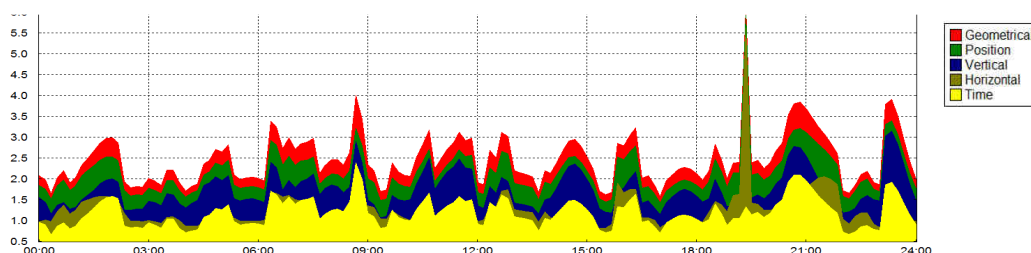- VDOP - vertical (height only),
- TDOP - time.

Fig. 3 Display of the development of all DOPs.

Adjustment of the geodetic network

A Gauss-Markov model (GMM) is the most frequently used method for 3D adjustment of a geodetic network as follows:

$$v = Ad\hat{C}\text{-}dL = Ad\hat{C}\text{-}(L-L°), \quad \text{- funkcionl part,}$$

$$\Sigma_L = s_0^2 Q_L, \quad \text{- stochastic part.} \tag{1}$$

230

The structure of individual values in the network is defined by m GNSS vectors obtained by observations, $n = 3m$, observation components, o fixed points, $l = 3o$ fixed parameters, b determined points $k = 3b$ and determined parameters [3, 4, 6, 7, 8]:

- Vector of observations $L_{(n,l)}$ is created by position coordinate differences between individual network points which are taken from the processing of vector in LGO 6.0 software. In order to obtain the current status using a UTCN 03 (Unified Trigonometric Cadastral Network 03) transformation key, the transformation of coordinates of fixed points and determined points from the ETRS 89 coordinate system into a UTCN 03 coordinate system was performed. The sequence of coordinate differences is given in alphabetical order of vector starting points based firstly on determined points and then on related points with coordinate differences ΔX, ΔY (UTCN) and elevations Δh (Baltic after Adjustment). This order is maintained for the entire adjustment.

- A vector of approximate coordinates of determined points $C^\circ_{(k,l)}$ is created by coordinates of determined points, which were taken from initial processing in LGO 6.0 software.

- A vector of approximate observations $L^\circ_{(n,1)}$ is given by relative coordinate differences of approximate coordinates of given points $L^\circ = f(C^\circ)$. The order of individual differences is the same as in L.

- The vector of auxiliary observation $dL_{(n,l)}$ is given by the difference of observation vector elements and the approximate observation vector $dL = L - L^\circ$ and is determined in millimetres.

- The cofactor matrix $Q_{L\,(n,n)}$ is a diagonal matrix with cofactors on the main diagonal. Cofactors are calculated using formula $q_i = \dfrac{\sigma_i^2}{\sigma_0^2}$, where $\sigma_0^2 = \dfrac{\Sigma \sigma_{\Delta X, \Delta Y}^2}{n}$, $\sigma_i = (5mm + 0.5\,ppm)$, whilst the producer states the accuracy of determination of vector lengths using a static method - 5mm + 0.5 ppm of length.

- Configuration matrix $A_{(n,k+l)}$ (partial derivations, design) characterises network geometry (configuration) of the network. This matrix was divided into an active part $A_{(n,k)}$ which will enter further adjustment, and a passive part $A_{(n,l)}$ which is allocated to o fixed points and is defined $A = \left(\dfrac{\partial f(C^\circ)}{\partial C^\circ} \right)_{C^\circ = \hat{C}}$. If vectors L° and C° are related to each other, the coefficients will have values $\{-1, 1\}$ and if not, they will have value $\{0\}$.

- Vector of estimates of auxiliaries of determined coordinates $d\hat{C}_{(k,l)}$ in mm was determined using a matrix multiplication: $d\hat{C} = (A^T Q_L^{-1} A)^{-1} A^T Q_L^{-1} (L - L^\circ) = N^{-1} A^T Q_L^{-1} dL$.

$$\tag{2}$$

- Adjusted coordinates of determined points $\hat{C}_{(k,1)}$ are determined: $\hat{C} = C^\circ + d\hat{C}$. $\tag{3}$

- Vector of corrections $v_{(n,1)}$ of observed values: $v = A d\hat{C} - dL$. $\tag{4}$

- Vector of adjusted measured values $\hat{L}_{(n,1)}$: $\hat{L} = L + v$. $\tag{5}$

- Estimated variance faktor $s_0^2{}_{(1,1)}$: $s_0^2 = \dfrac{v^T Q_L^{-1} v}{(n-k)}$. $\tag{6}$

- The covariance matrix $\Sigma_{\hat{C}\,(k,k)}$ of adjusted coordinates $\hat{X}_i, \hat{Y}_i$ is: $\Sigma_{\hat{C}} = s_0^2 Q_{\hat{C}}$. $\tag{7}$

- The covariance matrix $\Sigma_{\hat{L}\,(n,n)}$ of adjusted observations $\hat{L}$ is: $\Sigma_{\hat{L}} = s_0^2 Q_{\hat{L}}$. $\tag{8}$

Robust adjustment

The least square method (LSM) is the method generally used. It provides good results assuming that the measured values only contain random errors. If there are severe and systematic errors, these errors cannot be explicitly identified using corrections. Defects with the LSM led statistics to seek methods which are more resistant (robust) using remote measurement. Experiments have shown that robust estimates give better results than the LSM. The majority of robust adjustments used in geodesy modify the existing LSM to make it robust. When using the robust LSM, the weight of measurement changes in each iteration using the weight function. Remote measurements gradually obtain greater correction and therefore less weight, which eliminates their influence. After elimination of identified measurements, adjustment is carried out using the original weights. We know of two types of robust estimation: robust estimation applied to the LSM when the addition of corrective squares is replaced by more suitable corrective functions, and clearly robust methods which include Simplex and Friedrich methods.

When using the robust method for estimation, the minimised function $v^T v$ is replaced with the so-called loss function [2, 5]: $\rho(v_i) = \min$, which generates the influence function $\psi(v_i)$ characterising the influence of errors upon adjusted values. For this function, the following is valid:
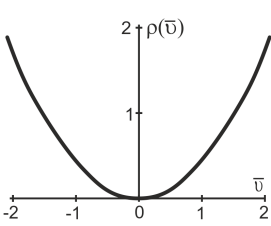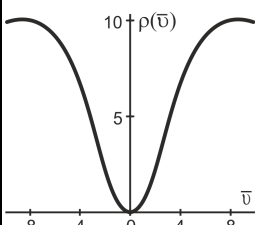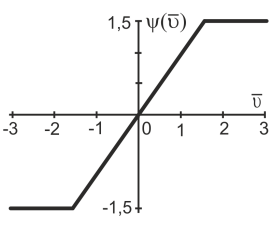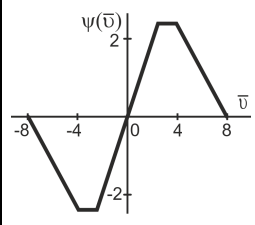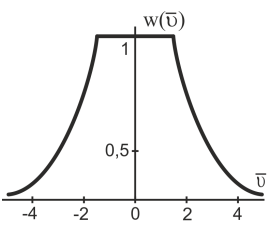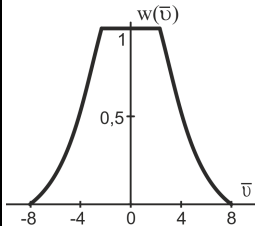
$$\sum_1^n \psi(v_i) = 0 , \qquad (9)$$

where $\psi(v_i) = \dfrac{\partial \rho(v_i)}{\partial v_i}$.

In order that the adjustment will have the nature of a robust estimate, it is suitable to carry it out using the iteration method with variable weighing, i.e. that the weight p_i of observation l_{ij} was determined in each iteration step as a corrective function: $p(v_i) = \psi(v_i)/v_i$, $\qquad (10)$

where $p(v_i)$ is the weight function.

The most used estimates are Huber's robust M-estimate, Hampel's robust M-estimate and Beweight's robust M-estimate, etc. The functions of selected estimates are shown in Tab. 2.

Tab. 2 Function of Huber's and Hampel's robust M-estimate.

	Huber's robust M-estimate		Hampel's robust M-estimate	
Loss function	$\rho(v_i) =$ $\begin{cases} \dfrac{1}{2} v_i^2 & \lvert v_i \rvert < k \\ k\lvert v_i \rvert - \dfrac{1}{2} k^2 & \lvert v_i \rvert \geq k \end{cases}$ Damping constant: k=1,5		$\rho(v_i) =$ $\begin{cases} \dfrac{1}{2} v_i^2 & \lvert v_i \rvert < a \\ a\lvert v_i \rvert - \dfrac{1}{2} a^2 & a \leq \lvert v_i \rvert < b \\ \dfrac{a}{2}\left(3b - a - c + \dfrac{(c - \lvert v_i \rvert)^2}{c - b}\right) & b \leq \lvert v_i \rvert < c \\ \dfrac{a}{2}(b - a + c) & c \leq \lvert v_i \rvert \end{cases}$ Damping constants: a=2, b=4, c=8;	
Influence function	$\psi(v_i) = \dfrac{\partial \rho(v_i)}{\partial v_i} =$ $\begin{cases} v_i & \lvert v_i \rvert < k \\ k\, sign(v_i) & \lvert v_i \rvert \geq k \end{cases}$		$\psi(v_i) = \dfrac{\partial \rho(v_i)}{\partial v_i} =$ $\begin{cases} v_i & \lvert v_i \rvert < a \\ a\, sing(v_i) & a \leq \lvert v_i \rvert < b \\ a\dfrac{c - \lvert v_i \rvert}{c - b} sing(v_i) & b \leq \lvert v_i \rvert < c \\ 0 & c \leq \lvert v_i \rvert \end{cases}$	
Corrective function	$p(v_i) = \dfrac{\psi(v_i)}{\lvert v_i \rvert}$ $\begin{cases} 1 & \lvert v_i \rvert < k \\ \dfrac{k}{\lvert v_i \rvert} & \lvert v_i \rvert \geq k \end{cases}$		$p(v_i) = \dfrac{\psi(v_i)}{\lvert v_i \rvert}$ $\begin{cases} 1 & \lvert v_i \rvert < a \\ \dfrac{a}{\lvert v_i \rvert} & a \leq \lvert v_i \rvert < b \\ a\dfrac{c - \lvert v_i \rvert}{(c - b)\lvert v_i \rvert} & b \leq \lvert v_i \rvert < c \\ 0 & c \leq \lvert v_i \rvert \end{cases}$	

Sighting network and evaluation of signals

By reconnaissance of the terrain of the Dargovských hrdinov suburbs, it was discovered that some points had been reconstructed and some were damaged. All points were stabilised as associated geodetic points (deep curbed bores reinforced with metal tubing and filled with concrete). On the surface of each pillar there is a concreted metal sheet with a drilled hole with a diameter of $\phi = 16\,\text{mm}$ which provides related centring, and a height marker is affixed to the lower part of the pillars (Fig. 4). As related points for adjustment, Haringeš, Varkapa and Široká (hereinafter: Her, Var, Šir) were used, stabilised by nail markers with small holes in stone joists with dimensions of 20 x 20 x 70 cm, protected with concreted shaft ring and protective bars (Fig. 5).

The selection of suitable determined points in risk areas depended upon the density of the built up area and greenery. Five determined points were selected, marked B-6, B-10, C-20, P-III-1, P-IV-1 (Fig. 6). When selecting this point, the possibility for the best possible reception of signals from the satellite was also considered.

Two types of receivers, Leica GPS900CS (Fig. 4) and Leica GPS1200 (Fig. 5), were used as well as a levelling device, Topcon DL-101C, allowing the performance of a levelling measurement using method of technical, accurate and very precise levelling as well as setting out.

Fig. 4 Observation at point C-20.

Fig. 5 Observation at point Široká.

The static method was chosen for measurement. Leica GPS1200 receivers were placed on fixed points Her, Var, Šir, where the sky was not obscured and a lower number of observed satellites (only GPS) were sufficient. Leica GPS900CS receivers were placed on determined points whilst a limited view of the sky was compensated by a greater number of observed satellites (GPS + Glonass).

A Leica GPS900CS was placed on determined points using a Zeiss base and two types of fixing screws. Horizontal levelling was carried out using pre-rectified optical centring device, inserted into the Zeiss base. Leica GPS1200 receivers were placed on tripods with three leg extensions at related points using a Zeiss pad and a special screw. During observation, the height difference of receiver aerials and the height marks of points was determined by a Topcon DL-101C levelling device using a levelling method. Leica Geo Office 6.0 (LGO) company software was using for processing measured data. This pre-processed data was used as input values when adjusting the LSM and robust methods.

The result of satellite measurements are vectors of coordinate differences $\Delta X_{ij}, \Delta Y_{ij}, \Delta h_{ij}$ between points of the geodetic network PB_i and PB_j (Fig. 7). They are generally influenced by disturbing factors, i.e. they are distorted by errors in the measurement method during its performance. For this purpose, components $\Delta X_{ij}, \Delta Y_{ij}, \Delta h_{ij}$ of all vectors determining the spatial area of points (structure of geodetic network) must undertake adjustment in order to create dispute-free geometry of a three dimensional geodetic network, i.e. determine an estimate of elements $\Delta \hat{X}_{ij} = \Delta X_{ij} + v_{\Delta Xij}$, $\Delta \hat{Y}_{ij} = \Delta Y_{ij} + v_{\Delta Yij}$, $\Delta \hat{h}_{ij} = \Delta h_{ij} + v_{\Delta hij}$ in satellite vectors and at the same time, determine the levelled coordinates $\hat{X}_i, \hat{Y}_i, \hat{h}_i$ of points PB.
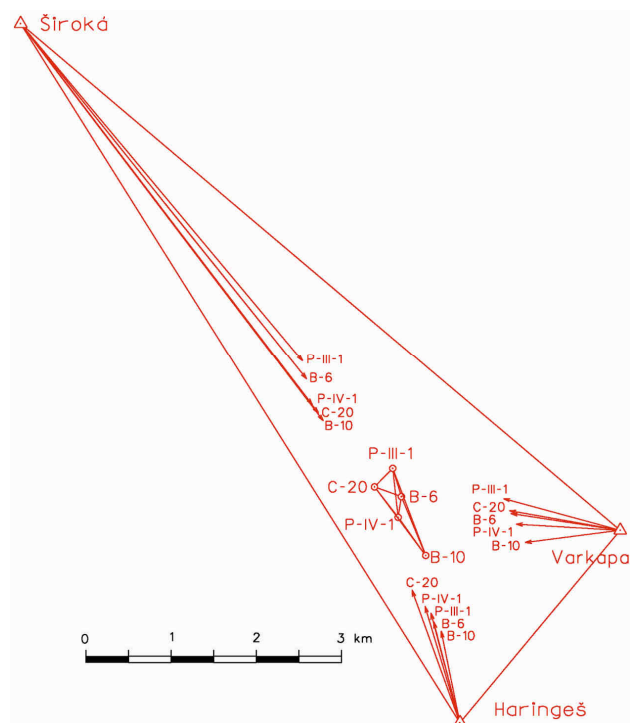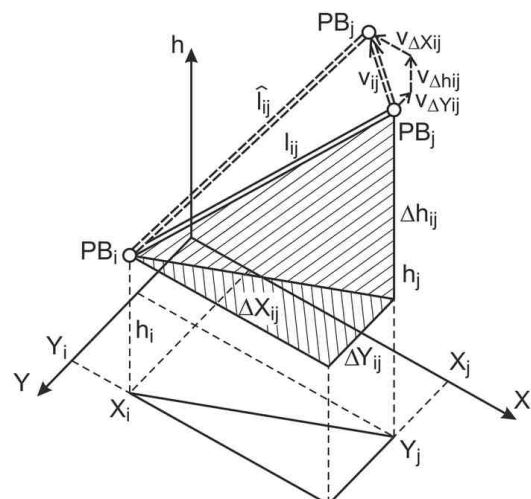

Fig. 6 Geodetic network situation.

Fig. 7 Coordinate components of GNSS vector.

Gauss Markov model with full rank of the network

For 3D Gauss Markov model with full rank of GNSS observations GMM, spatial coordinates of five determined points and three fixed points were used as well as coordinate difference between them (Fig. 6). The structure of individual values in this network is defined by $m = 28$ GNSS vectors obtained by observations, $n = 3m = 84$ observation components, $b = 5$ determined points and $k = 3b = 15$ determined parameters: vector of observations $L_{(84,l)}$, vector of approximate coordinates of determined points $C^{\circ}_{(15,l)}$, vector of approximate coordinates $L^{\circ}_{(84,l)}$, vector of auxiliary observations $dL_{(84,l)}$, cofactor matrix $Q_{L(84,84)}$, configuration matrix $A_{(84,24)}$ with active part $A_{(84,15)}$, vector of estimates of auxiliaries to determined coordinates $d\hat{C}_{(15,l)}$, vector of adjusted coordinates of determined points $\hat{C}_{(15,l)}$, vector of corrections of observed values $v_{(84,l)}$, vector of adjusted measured values $\hat{L}_{(84,1)}$, estimated variance factor $s_0^2{}_{(1,1)}$, covariance matrix of adjusted coordinates $\Sigma_{\hat{C}(15,15)}$, covariance matrix of adjusted values of observed values $\Sigma_{\hat{L}(84,84)}$. Adjustment of observations is not part of the article due to its size.

Tab. 3 Estimates of unknown parameters (UTCN 03): 1 - LSM, 2 - Huber's robust M-estimate, 3 - Hampel's robust M-estimate.

Order No.	Coordinates of points		$C^{\circ}_{UTCN-03}$ [m]	$d\hat{C}$ [mm]			$\hat{C}_{UTCN-03}$ [m]			$\sigma_{\hat{C}}$ [mm]		
				1	2	3	1	2	3	1	2	3
1	B-6	X	1238170.732	-0.28	-0.20	-0.38	1238170.732	1238170.732	1238170.732	0.75	0.53	0.53
2		Y	261135.927	0.38	0.32	0.29	261135.927	261135.927	261135.927	0.75	0.55	0.51
3		h	245.928	1.42	1.02	1.25	245.929	245.929	245.929	0.60	0.63	0.55
4	B-10	X	1238862.015	0.21	0.24	0.11	1238862.015	1238862.015	1238862.015	0.76	0.53	0.54
5		Y	260850.322	0.56	0.53	0.49	260850.323	260850.323	260850.322	0.75	0.56	0.52
6		h	280.320	0.75	0.38	0.44	280.321	280.320	280.320	0.60	0.57	0.47
7	C-20	X	1238054.795	-0.03	-0.07	-0.13	1238054.795	1238054.795	1238054.795	0.76	0.53	0.53
8		Y	261450.467	-0.38	-0.41	-0.41	261450.467	261450.467	261450.467	0.77	0.53	0.53
9		h	218.218	0.24	-0.12	0.03	218.218	218.218	218.218	0.61	0.59	0.49
10	P-III-1	X	1237837.321	-0.36	-0.26	-0.46	1237837.321	1237837.321	1237837.321	0.77	0.53	0.54
11		Y	261238.302	0.59	0.47	0.57	261238.303	261238.302	261238.303	0.75	0.53	0.52
12		h	260.130	0.04	-0.27	-0.15	260.130	260.130	260.130	0.60	0.62	0.53
13	P-IV-1	X	1238412.354	-1.27	-1.30	-1.56	1238412.353	1238412.353	1238412.352	0.75	0.57	0.54
14		Y	261173.393	-0.39	-0.18	-0.35	261173.393	261173.393	261173.393	0.75	0.55	0.51
15		h	265.163	-0.91	-1.21	-1.17	265.162	265.162	265.162	0.60	0.61	0.50

Tab. 3 shows approximate and adjusted coordinates of five determined points together with accuracy of adjusted coordinates $\sigma_{\hat{C}}$. The dimension of individual vectors is (15,1). In robust M estimates, higher accuracy of adjusted coordinates $\sigma_{\hat{C}}$ was achieved in comparison with the LSM. This is proven by the lower values. After adjustment of measured values, it is necessary to verify, by statistic testing, whether the vector of measured values does not contain measurements with serious errors (remote measurement).

Testing the geodetic network and graphic visualisation

The adjusted network structure was tested using various methods. Suitability of selection of GMM used for adjustment was verified by a global test of an estimating model and the presence of remote measurements was tested by a Student and Pope test.

In the global test, test statistics given by the calculation $T_G = s_0^2(n-k)/\sigma_0^2$ was compared with the critical value with division χ^2 (chi-Square) at the level of significance $\alpha = 0,05$ and grades of freedom $f = (n-k)$ $T_{KRIT} = \chi_{\alpha}^2(n-k)$, where $n = 3m = 84$ represents the number of observation components and $k = 3b = 15$ represents the number of determined parameters.

In all adjustments there is $T_{KRIT}(\chi_{\alpha}^2) > T_G$ (Tab. 4), the test did not confirm discrepancies between the mathematical model of adjustments and observations; therefore it can be considered as undistorted and the observation can be considered to be without serious errors [1]. Identification tests did not confirm the presence of a remote measurement or any serious error in the observations, and none of the values were excluded (Tab. 4).

Tab. 4 Testing the observation of the geodetic network.

Global test		LSM						Huber's robust M-estimate						Hampel's robust M-estimate					
Global test		$T_G = 2.67 < T_{KRIT} = 3.91$						$T_G = 1.40 < T_{KRIT} = 2.91$						$T_G = 1.31 < T_{KRIT} = 3.91$					
Localization test		Student test			Pope test			Student test			Pope test			Student test			Pope test		
Order No.	GNSS vector	$T_{KRIT} =$ 3.98			$T_{KRIT} =$ 3.32			$T_{KRIT} =$ 3.96			$T_{KRIT} =$ 3.34			$T_{KRIT} =$ 3.98			$T_{KRIT} =$ 3.32		
	A_i / A_{i+1}	T_X	T_Y	T_h	T_X	T_Y	T_h	T_X	T_Y	T_h	T_X	T_Y	T_h	T_X	T_Y	T_h	T_X	T_Y	T_h
1	B-6 B-10	0.34	0.24	0.26	0.35	0.25	0.26	0.42	0.28	0.36	0.39	0.26	0.33	0.50	0.33	0.23	0.50	0.33	0.23
2	B-6 C-20	0.61	0.20	0.94	0.61	0.20	0.94	0.85	0.22	1.15	0.78	0.20	1.05	0.87	0.21	1.46	0.87	0.22	1.46
3	B-6 P-III-1	0.32	0.17	2.12	0.33	0.17	2.08	0.42	0.14	1.91	0.39	0.13	1.72	0.46	0.32	1.84	0.47	0.32	1.81
4	B-6 P-IV-1	0.39	0.19	0.53	0.39	0.19	0.53	0.59	0.49	0.77	0.54	0.45	0.71	0.76	0.42	0.70	0.76	0.42	0.71
5	B-10 C-20	0.53	0.04	0.38	0.53	0.04	0.38	0.67	0.06	0.50	0.61	0.05	0.46	0.75	0.10	0.69	0.75	0.10	0.69
6	B-10 P-III-1	0.37	0.35	1.77	0.38	0.36	1.75	0.48	0.55	1.73	0.44	0.51	1.57	0.54	0.45	1.60	0.54	0.46	1.59
7	B-10 P-IV-1	0.39	0.80	2.74	0.39	0.80	2.65	0.45	1.26	2.08	0.42	1.15	1.88	0.36	1.27	1.95	0.36	1.27	1.91
8	C-20 P-III-1	0.26	0.02	0.15	0.26	0.02	0.15	0.18	0.12	0.16	0.17	0.11	0.15	0.37	0.03	0.21	0.38	0.03	0.21
9	C-20 P-IV-1	0.20	0.39	0.67	0.20	0.40	0.67	0.27	0.26	0.90	0.25	0.24	0.83	0.08	0.49	0.93	0.08	0.49	0.93
10	P- P-IV-1	0.30	0.42	0.44	0.30	0.42	0.44	0.53	0.83	0.57	0.48	0.76	0.52	0.62	0.68	0.57	0.62	0.68	0.58
11	B-6 Her	0.13	0.42	3.49	0.13	0.42	3.28	0.18	0.63	2.21	0.17	0.58	1.98	0.26	0.68	2.02	0.26	0.69	1.98
12	B-6 Šir	0.09	0.90	3.07	0.09	0.90	2.92	0.18	1.68	2.33	0.17	1.53	2.08	0.18	1.63	2.36	0.18	1.62	2.29
13	B-6 Var	0.20	0.30	1.44	0.20	0.30	1.43	0.18	0.63	1.45	0.17	0.58	1.32	0.40	0.49	1.37	0.40	0.49	1.36
14	B-10 Her	0.11	0.41	0.56	0.11	0.41	0.56	0.22	0.49	0.35	0.20	0.45	0.33	0.08	0.50	0.47	0.08	0.50	0.48
15	B-10 Šir	0.09	1.12	0.54	0.09	1.12	0.54	0.24	1.91	1.05	0.22	1.72	0.96	0.18	1.87	1.12	0.18	1.84	1.12
16	B-10 Var	0.16	0.47	0.94	0.16	0.47	0.94	0.22	0.90	0.82	0.20	0.83	0.75	0.11	0.72	1.02	0.11	0.73	1.03
17	C-20 Her	0.01	0.24	2.05	0.01	0.25	2.02	0.07	0.38	1.72	0.06	0.35	1.56	0.09	0.37	1.62	0.09	0.37	1.61
18	C-20 Šir	0.16	0.44	2.39	0.16	0.44	2.33	0.39	1.01	2.09	0.36	0.92	1.88	0.18	0.61	2.14	0.18	0.61	2.10
19	C-20 Var	0.02	0.41	1.29	0.02	0.41	1.29	0.07	0.84	1.31	0.06	0.77	1.20	0.13	0.60	1.69	0.14	0.60	1.68
20	P- Her	0.62	0.39	0.77	0.62	0.39	0.78	1.17	0.43	0.69	1.07	0.39	0.64	0.95	0.53	0.95	0.95	0.53	0.96
21	P- Šir	0.05	0.61	2.57	0.05	0.61	2.49	0.22	1.36	2.14	0.20	1.24	1.92	0.02	0.85	2.20	0.02	0.85	2.14
22	P- Var	0.43	0.19	1.93	0.44	0.19	1.90	0.68	0.49	1.68	0.62	0.45	1.53	0.52	0.29	1.58	0.52	0.30	1.56
23	P-IV- Her	0.61	0.07	1.05	0.61	0.07	1.05	1.12	0.29	1.52	1.03	0.27	1.38	0.66	0.14	1.87	0.67	0.14	1.85
24	P-IV- Šir	1.75	0.91	2.94	1.73	0.91	2.81	3.18	1.64	2.96	2.76	1.49	2.59	0.92	1.68	2.03	0.92	1.66	1.98
25	P-IV- Var	0.56	0.67	0.30	0.56	0.67	0.30	0.65	1.10	0.68	0.60	1.00	0.62	0.49	0.92	0.74	0.49	0.92	0.75
26	Her Šir	0.00	0.00	0.00	0.00	0.00	0.00	0.00	0.00	0.00	0.00	0.00	0.00	0.00	0.00	0.00	0.00	0.00	0.00
27	Her Var	0.24	0.00	0.68	0.24	0.00	0.69	0.42	0.00	0.84	0.39	0.00	0.77	0.34	0.00	0.98	0.34	0.00	0.98
28	Šir Var	0.16	0.71	0.66	0.16	0.71	0.67	0.42	1.65	0.84	0.39	1.49	0.77	0.22	1.64	0.95	0.22	1.62	0.95

On the basis of the results of processing and adjustment (LSM and 2x robust – Tab. 3), graphic visualisation of the 3D geodetic network was created (Fig. 8) using absolute confidence ellipsoids. These are situated at observed points in UTCN 03. Graphic visualisation and source code of adjustment were created in a MatLab 2010 software environment. Adjustment of the geodetic network using LSM provides results with accuracy lower than Huber's or Hampel's robust M-estimates. This is proven by output values $\sigma_{\hat{C}}$ (Tab. 3), as well as the sizes of absolute ellipsoids (Fig. 8).
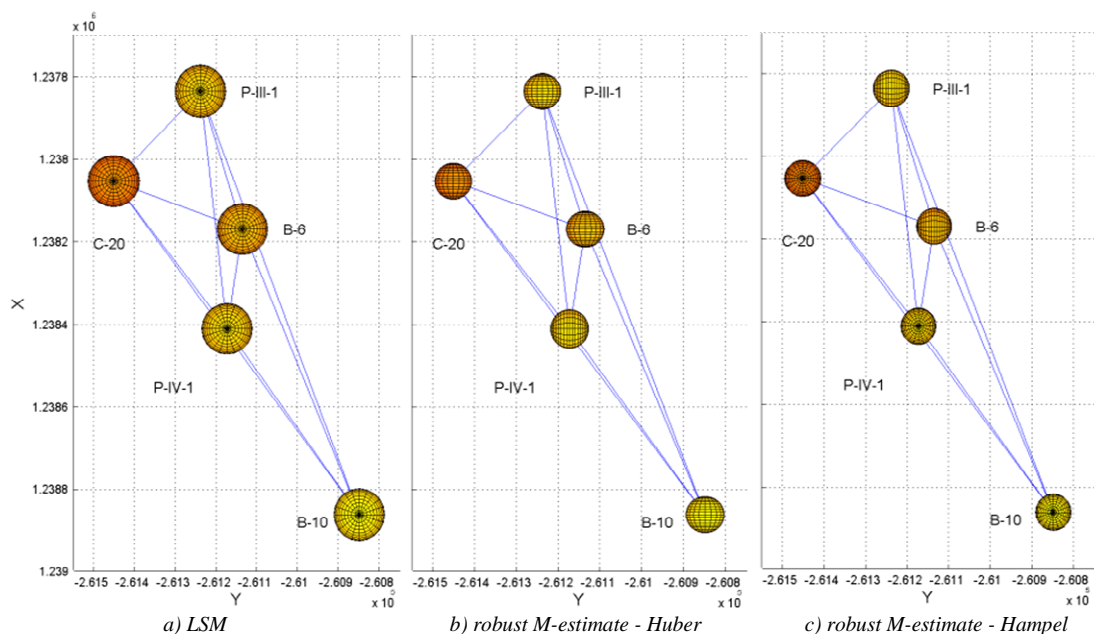

a) LSM   b) robust M-estimate - Huber   c) robust M-estimate - Hampel
Fig. 8 Visualisation of 3D adjustment of the geodetic network.

Fig. 9 to Fig. 11 represents graphic visualisation of absolute confidence ellipsoids at observed points. The centres of ellipsoids are adjusted coordinates $\hat{C}$ of determined points. Marking individual axes X, Y, h is amended by a lower case character r meaning reduced coordinates. For clarity and legibility, reduced coordinates of determined points, created by crossing off all figures before the decimal point, are displayed on the axes. The direction of an axis is displayed so the direction of the axis was as in UTCN 03, i.e. the positive direction of axis in a southerly direction and the positive direction of axis in a westerly direction (Fig. 8), or approximately in that direction (Fig. 9 to Fig. 11).
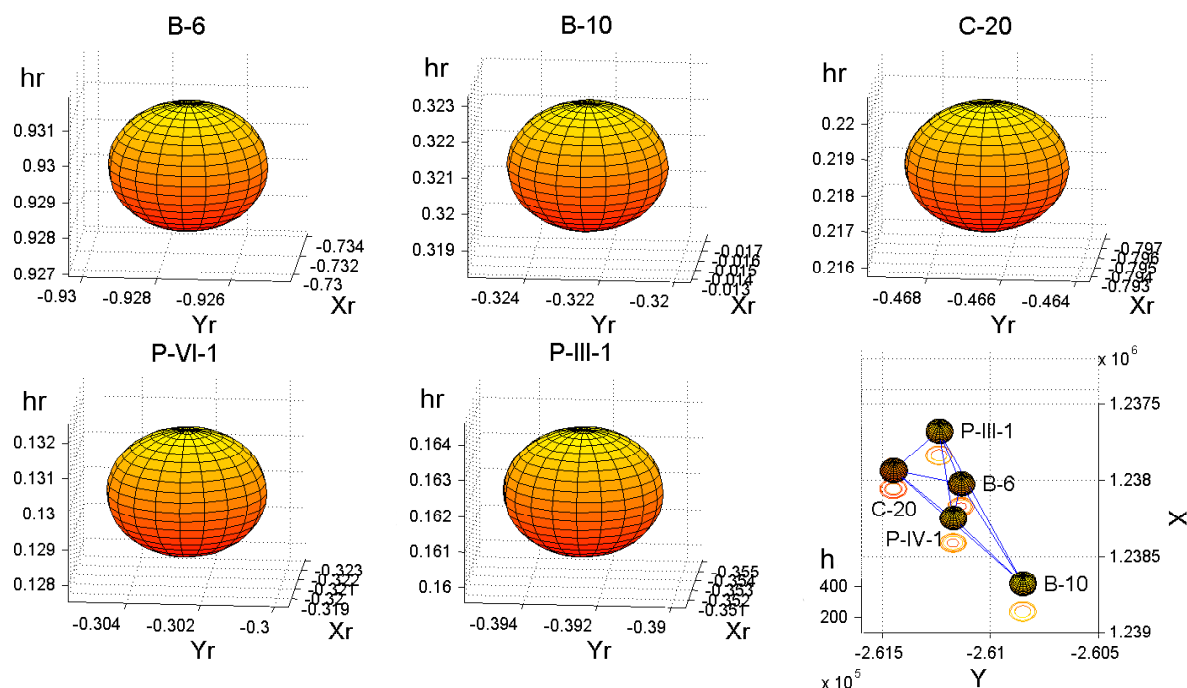

Fig. 9 Visualisation of adjustment using the LSM by absolute confidence ellipsoids.
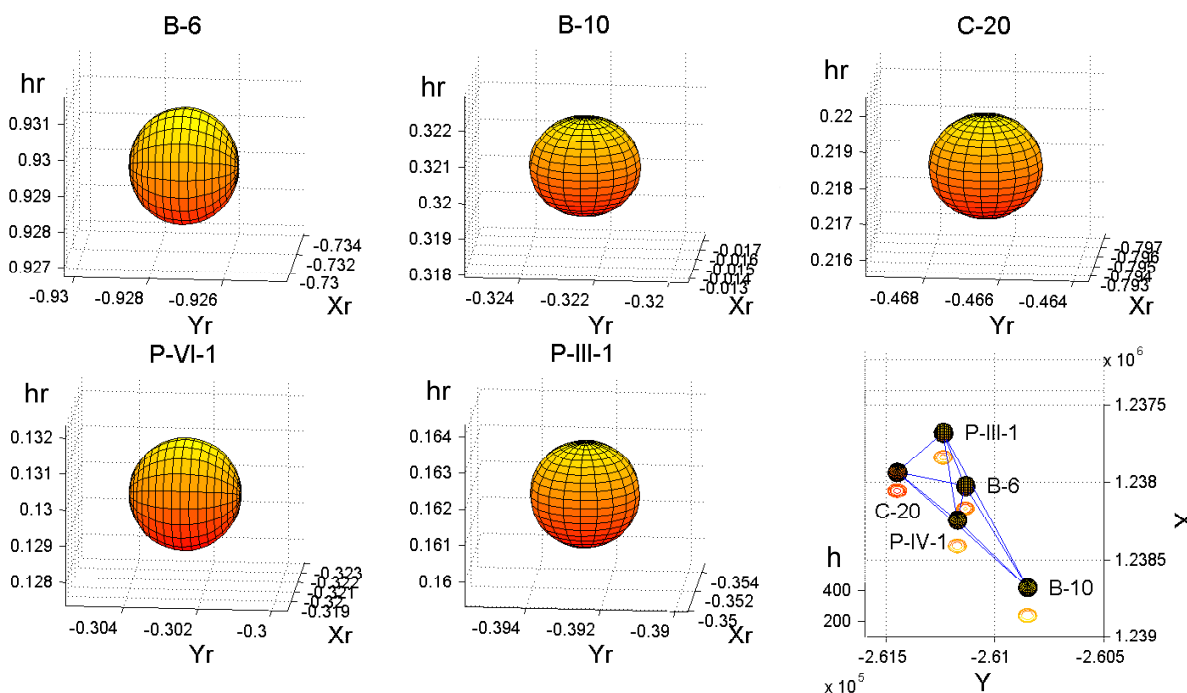

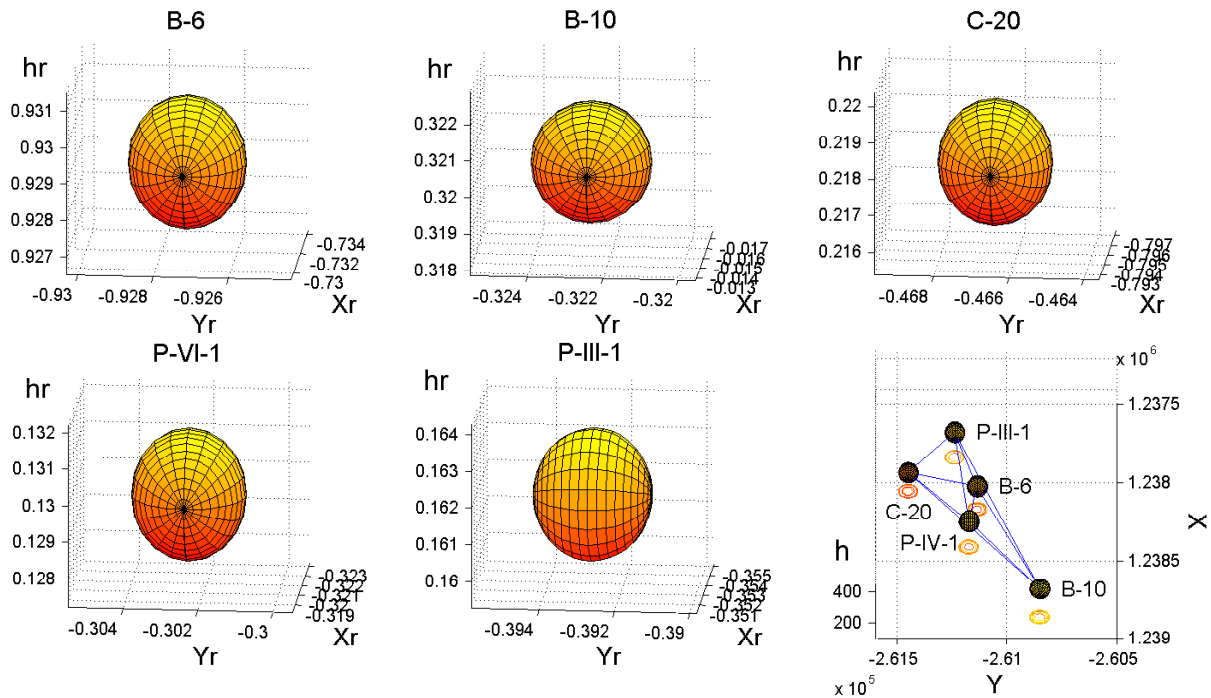*Fig. 10 Visualisation of adjustment by Huber's robust M-estimate by absolute confidence ellipsoids.*

Fig. 11 Visualisation of adjustment by Hampel's robust M-estimate by absolute confidence ellipsoids.

Summary

Using GNSS technology is preferred for observation of a 3D geodetic network for the purposes of deformation analysis. In order to achieve maximum accuracy of observations, planning GNSS observations is also important. Gauss Markov model with full rank of GNSS observations in a geodetic network was carried out using the Gauss-Markov model. Adjustment of the 3D geodetic network using LSM provides estimates for unknown parameters with accuracy lower than Huber's or Hampel's robust M-estimates. This is proven not only by adjusted estimates of unknown parameters in Tab. 3, but also by graphic visualisation of adjustment methods using absolute confidence ellipsoids (Fig. 8 to Fig. 11). The whole network is visualised together as well as individual observed network points separately.

References

[1]   Caspary, W. F.: Concepts of network and deformation analysis. *First edition. Kensingthon: School of surveying The University of New South Wales, 1987. 187, ISBN 0-85839-044-2.*

[2]   Gašincová, S., Gašinec, J., Trembeczká, E.: Adjustment of 2D geodetic networks using robust methods. *In: Geodesy, cartography and geographic information systems 2008: 5. Scientific-specialist conference with international participation: 16.-19. September 2008, Vysoké Tatry - Stará Lesná. Košice: GK a GIS 2008, 8, ISBN 978-80-553-0079-5.*

[3]   Gašincová, S., Kňežo D., Mixtaj, L., Harman P.: Impact measuring and Numerical errors in LSM adjustment of Local Geodetic Net. *GeoScience Engineering, 2011, Volume LVII, Issue No.1, ISSN 1802-5420.*

[4]   Labant, S.: Monitoring landslide areas in real-time. *PhD thesis, TU Košice, F BERG, 2008, 147.*

[5]   Jäger, R., Müller, T. Saler, H., Schwäble, R.: Klassische und Robuste Ausgleichungsverfahren. *Wichmann, Heidelberg, 2005. 340, ISBN 3-87907-370-8.*

[6]   Pukanská, K., Weiss, G.: Precision the points position with use technology GPS *In: Coal - Ores - Geological Exploration. 14, 2007, 9, 30-35, ISSN 1210-7697.*

[7]   Sabová, J., Jakub, V.: Geodetic deformation monitoring. *First edition. Košice: Editor centre and editorial office AMS, F BERG, Technical University of Košice, 2007. 128, ISBN 978-80-8073-788-7.*

[8]   Weiss, G., Gašinec, J., Engel, J., Labant, S., Rákay, Š.: Effect incorrect points of the Local Geodetic Network at results of the adjustment. *Acta Montanistica Slovaca, 13, 2008, 4, 485-490, ISBN 1335-1788.*

[9]   http://www.trimble.com/planningsoftware_ts.asp (online), (Cited 2010.3.20).

[10]   http://freegeographytools.com/2007/determining-local-gps-satellite-geometry-effects-on-position-accuracy (online), (Cited 2010.3.20).